Increased endothelial cell selectivity of triazole-bridged dihalogenated A-ring analogues of combretastatin A–1

Thomas M. Beale [a], Peter J. Bond [b], James D. Brenton [c], D. Stephen Charnock-Jones [d], Steven V. Ley [a], Rebecca M. Myers [a,*]

[a] Department of Chemistry, Lensfield Road, University of Cambridge, Cambridge CB2 1EW, United Kingdom
[b] Unilever Centre for Molecular Science Informatics, Lensfield Road, University of Cambridge, Cambridge CB2 1EW, United Kingdom
[c] Functional Genomics of Ovarian Cancer Laboratory, Cancer Research UK, Cambridge Research Institute, Li Ka Shing Centre, Robinson Way, Cambridge CB2 0RE, United Kingdom
[d] Department of Obstetrics and Gynaecology, University of Cambridge and National Institute for Health Research, Cambridge Comprehensive Biomedical Research Centre, Cambridge CB2 0SW, United Kingdom

ARTICLE INFO

ABSTRACT

The antiproliferative activity on ovarian cancer (SK-OV-3) cells of a series of triazole-bridged combretastatin analogues (**37**, **38**, **40–43**) containing dihalogenation of the A-ring is reported, and compared with their trimethoxy analogues (**5**, **15**, **39**). It was found that dihalogenation with either bromine or iodine was a tolerated modification when compared to the parent compound combretastatin (CA–4, **1**) and had less effect than B-ring modification on potency. These compounds exhibited G_2/M arrest, and maintained antitubulin activity. Further assays on human umbilical vein endothelial cells (HUVECs) demonstrated the potential antivascular effects of these triazoles. Of particular note was a 3,5-diiodo-4-methoxyaryl triazole (**43**) which had promising 7-fold selectivity for HUVECs over ovarian cancer cells.

© 2012 Elsevier Ltd. All rights reserved.

1. Introduction

Vascular disrupting agents (VDAs) are a relatively new group of targeted therapies that are under active clinical, biological and chemical investigation.[1] The water-soluble prodrugs combretastatin A-4 phosphate (CA–4P, **2**), combretastatin A-1 diphosphate (CA–1P, **4**) and AVE8062 (Ombrabulin) are three such promising VDA candidates for the treatment of cancer (Fig. 1).[2] These *cis*-stilbenes originate from the naturally-occurring 3-hydroxylated CA–4 (**1**) and 2,3-dihydroxylated CA–1 (**3**) combretastatin family of plant-based lignans.[3] Despite the efficacy of CA–4P (**2**) in being able to induce cell death in the core of a tumour by collapsing the network of tumour blood vessels, it is less effective in eradicating cells in the tumor rim where blood can be supplied by nearby non-tumour vasculature. Furthermore, there is evidence that **2** causes elevated blood pressure,[4] and the potential for pharmacologic and adverse toxicity interactions between VDAs, including **2**, when used in combination with traditional chemotherapy has also been reported.[5]

Our interests lie in the potential application of vascular disrupting agents to the treatment of ovarian cancer. This is due to the highly vascularised nature of epithelial ovarian cancer, coupled with the very poor prognosis of patients who have failed front-line treatment.[6]

When we explored the relevant VDA literature, we found a 3,4,5-trimethoxyaryl A-ring to be a recurring structural theme.[7] This moiety is generally believed to be essential for biological activity, although we found the evidence to support this is somewhat sparse and incomplete. Since the trimethyoxyaryl A-ring is common to several other antimitotic agents (colchicine, podophyllotoxin and steganacin) that also bind at the colchicine binding site,[8] it may have been presumed to be a privileged scaffold important for effective binding. We have recently reported that this is not the case and equivalent potency can be achieved via dihalogenation of the A-ring in *cis*-stilbene analogues of **1** and **3**.[9]

However, due to the poor aqueous solubility and relative chemical instability of many *cis*-stilbenes, 5-membered heterocycles, including triazoles, have been widely explored as alternative bridging groups.[10] There are two distinct families of triazoles, those that possess three contiguous nitrogens (1,2,3-triazoles) and those with two (1,2,4-triazoles). Together they offer a variety of regioisomers with respect to the A- and B-rings; their connectivity through nitrogen or carbon and 1,4- or 1,5-geometry.[11]

The relative position of the nitrogen atoms in 1,2,3-triazole analogues of **1** have been shown to influence biological activity (Fig. 2).

* Corresponding author.
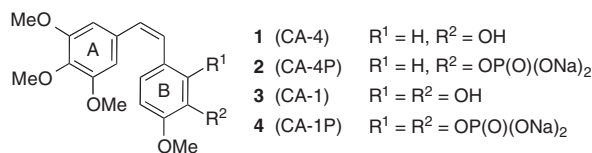 E-mail address: rmm32@cam.ac.uk (R.M. Myers).

Figure 1. Structures of naturally-occurring CA–4 (**1**) and CA–1 (**3**) and their corresponding phosphate prodrugs **2** and **4**.

Compounds where the A-ring was linked via nitrogen (e.g. **5** and **6**) were 10- to 50-fold more active than compounds with B-ring nitrogen connectivity (**7** and **8**).[12] This observation was reinforced by the screening results of a further triazole collection, where nitrogen connectivity was also shown to be important.[13] Furthermore, changing the 1,5-geometry of **6** to the 1,4-regioisomer **9** resulted in a 100-fold drop in activity (IC$_{50}$ = 11 nM for **6** to IC$_{50}$ = 1300 nM for **9**) (Fig. 2).[12]

In other studies, methylene units have been added between the aryl groups and the triazole bridge producing compounds that were at least 35-fold less active[14] and moderate micromolar activity was reported for compounds where the aryl groups were both linked through carbon (e.g. **10**).[15]

A more complex picture emerges for 1,2,4-triazole bridged analogues of **1**. Triazole **11** with 1,5-geometry and the A-ring attached via carbon and the B-ring via nitrogen, most closely resembling **1**, was found to be cytotoxic (IC$_{50}$ = 25–544 nM) across the 5 cancer cell lines that were tested.[16] It also had anti-tubulin activity (IC$_{50}$ = 6 μM). However, we found interesting correlations between **12**, **13** and **14** in this and another report.[17] The second study suggested that the relative positions of the aryl rings made a significant difference to antiproliferative activity. Compounds in which the A-ring was attached via carbon were largely inactive (e.g. **14**, IC$_{50}$ > 10 μM) when compared to the analogous compound where the two rings had been transposed (e.g. **13**, IC$_{50}$ = 280 nM). In contrast to **14**, triazole **12** (IC$_{50}$ = 290 nM) was also active in the same cell line (HeLa).[16] Taken together, the data from these two reports suggest that the connectivity of the two rings perhaps matters less than the pattern of the nitrogen atoms in the triazole. Unfortunately, the remaining isomeric triazole to complete this series has not been reported. However, in all cases, switching the rings from 1,5- to 1,4-geometry in 1,2,4-triazoles results in large reductions in potency.[18]

Following the submission of this manuscript, a 1,2,3-triazole combretastatin analogue containing a combretastatin A-1 B-ring (**15**) was reported, alongside other disubstituted B-ring analogues,

all containing a trimethoxy A-ring.[19] This analogue exhibited low micromolar activity in an angiogenesis assay and against human cancer cells.

Our interest in 3,5-dibromotyrosine-derived marine natural products (e.g. subreamollines, bromoverongamine and the antimitotic ceratamines)[20] led us to look initially at A-ring halogenation of CA-4 (**1**). We subsequently found that 3,5-dibromination and 3,5-diiodination of the A-ring in **1** increases growth inhibition of cancer cell lines and primary human umbilical vein endothelial cells (HUVECs).[9] This potency was achieved whilst maintaining cellular antitubulin activity and increasing the levels of G$_2$/M arrest from 31% (**1**, OMe) to 54% (Br) and 84% (I) respectively. However, chemical instability proved to be a problem with these compounds. Given that biological activity was previously maintained for 1,2,3-triazole bridged analogues of combretastatin, we targeted dihalogenated triazoles in an effort to examine the effects of dihalogenation in more detail.

Shortly after our report of dihalogenated CA–4 analogues, A-ring mono-halogenated (chlorine or bromine) methylimidazole-bridged CA–4 analogues[21] were also shown to have improved potency over their direct trimethoxy analogue.[22] This was followed by a recent report of similar mono- and di-halogenated methylimidazole-bridged analogues, which demonstrated that dihalogenation gave superior activity than monohalogenated analogues, though the direct trimethoxy analogue for comparison was not reported.[23]

In the work described here, we discuss our findings on A-ring dihalogenation of triazole analogues of **1** and **3**. We also examine what effect changes to the B-ring have on potency in combination with our novel scaffold. As the vast majority of related analogues possess a trimethoxy A-ring, these analogues were also synthesised as reference compounds. Therefore, we targeted compounds containing trimethoxy, dibrominated and diiodinated A-rings, alongside 2- and 3-hydroxylated and 2,3-dihydroxylated B-ring motifs, connected via a 1,2,3-triazole bridge. Building upon previously reported structure–activity relationships (vide supra), we limited this to A-rings linked to the triazole via nitrogen and possessing 1,5-geometry.

2. Results and discussion

2.1. Chemical synthesis

Our general approach for the synthesis of the triazoles was to perform a Huisgen cycloaddition using A-ring azides and B-ring alkynes, using a magnesium Grignard reagent to enforce the desired
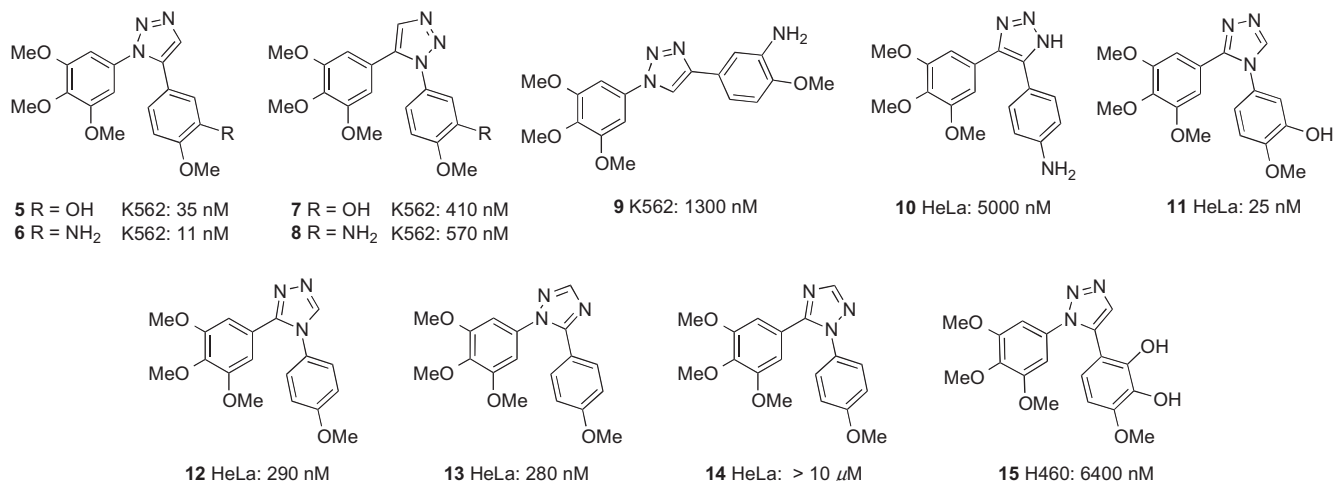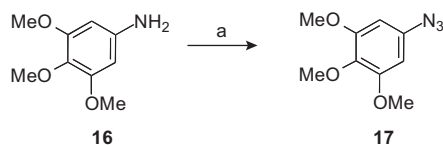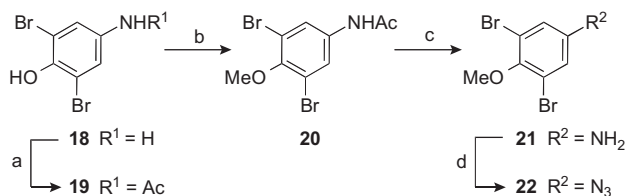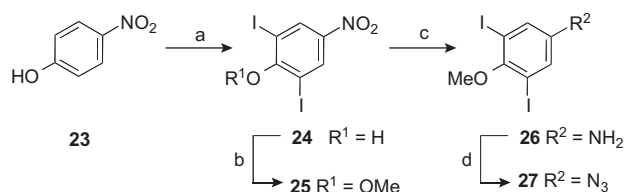

Figure 2. Triazole analogues of CA–4; 1,2,3-triazoles (**5–10**), 1,2,4-triazoles (**11–14**) and recently reported CA–1 analogue **15**. IC$_{50}$ values on the cell line indicated are shown.

Scheme 1. Reagents and conditions: Preparation of 3,4,5-trimethoxyaryl azide **17**. (a) (i) NaNO$_2$, H$_2$O/HCl (1:1), 0 °C; (ii) NaN$_3$, H$_2$O, 0 °C to rt, 2 h, 84%.

Scheme 2. Reagents and conditions: Synthesis of 3,5-dibromo-4-methoxyaryl azide **22**. (a) Ac$_2$O, AcOH, rt, 30 min, 98%; (b) MeI, K$_2$CO$_3$, acetone, 120 °C, μW, 30 min, 83%; (c) 3 m HCl, 140 °C, μW, 10 min, 95%; (d) (i) NaNO$_2$, H$_2$O/HCl (1:1), 0 °C; (ii) NaN$_3$, H$_2$O, 0 °C to rt, 2 h, 91%.
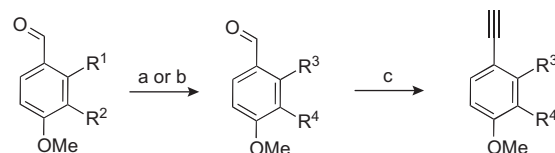

Scheme 3. Reagents and conditions: Synthesis of 3,5-diiodo-4-methoxyaryl azide **27**. (a) NaClO$_2$, NaI, HCl, MeOH/H$_2$O, 0 °C to rt, 18 h, 94%; (b) K$_2$CO$_3$, (MeO)$_2$SO$_2$, acetone, 65 °C, 18 h, 87%; (c) SnCl$_2$, EtOH/EtOAc, 70 °C, 2 h, 79%; (d) (i) NaNO$_2$, H$_2$O/HCl (1:1), 0 °C; (ii) NaN$_3$, H$_2$O, 0 °C to rt, 2 h, 96%.

Scheme 4. Reagents and conditions: (a) TBSCl, Et$_3$N, DMF, 18 h, rt, **31** quant., **32** 68%; (b) TBSCl, Et$_3$N, DMAP, rt, **33**, 96%; (c) 0.1 m LDA, THF, −78 °C, TMS-diazomethane, 1 h, then aldehyde, 1 h, 0 °C to rt, **34** 74%, **35** 52%, **36** 64%.

of the phenol groups proceeded in quantitative yield for **31** and in 68% and 96% for **32** and **33**. The aldehydes were readily converted to the corresponding alkynes **34–36** using trimethylsilyl diazomethane and lithium diisopropylamide in reasonable yields (74%, 52% and 64% respectively).[24]
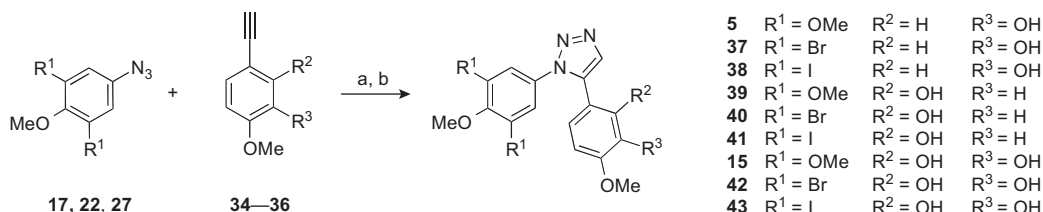
Triazoles **5**, **15** and **37–43** were formed from the various A-ring and TBS-protected B-ring components via Huisgen cycloaddition (Scheme 5 and Table 1).[12] Pre-complexation of the alkyne with EtMgCl followed by addition of the azide afforded exclusively the desired 1,5-geometry of the aryl groups. In general, lower yields were obtained when the ruthenium catalyst, RuCp*(PPh$_3$)$_2$Cl which has been reported to give selective 1,5-triazole products was used, as small amounts of the 1,4-triazole was formed during the reaction.[28] Deprotection of the cycloaddition products with TBAF afforded **5**, **15** and **37–43** in variable yields (Scheme 5 and Table 1).

2.2. Biological evaluation

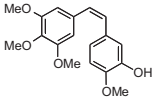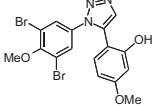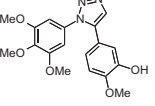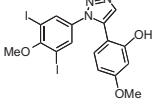#### 2.2.1. In vitro cell growth inhibition
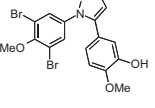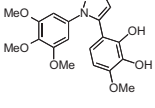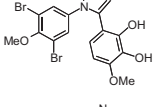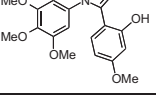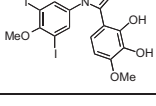
The triazole series (**5**, **15**, **37–43**) were tested in growth inhibition assays on an ovarian cancer cell line (SK-OV-3) using CA–4 (**1**) as a reference compound. The results are reported in Table 1. The MTS and sulforhodamine B (SRB) assays were both performed on the SK-OV-3 cell line using three replicate experiments, as differences between compounds were difficult to resolve (Table 1). In summary, all nine triazoles had potent nanomolar activity (IC$_{50}$ = 0.9–32.4 nM) compared to reference compound **1** (IC$_{50}$ = 1.7 nM). The results were consistent across both assays with small confidence intervals (CI).

Taking the B-ring as the fixed point for comparison and data from the SRB assay, the strongest antiproliferative effects were obtained for **5**, **37** and **38** containing the natural 3-hydroxy-4-methoxyaryl B-ring (as in **1**) (IC$_{50}$ = 0.9–2.4 nM). Switching the A-ring from 3,4,5-trimethoxyaryl (**5**) to 3,5-dibromo-4-methoxyaryl (**37**) or 3,5-diiodo-4-methoxyaryl (**38**) resulted in only a 2-fold loss of activity (IC$_{50}$ values: **37**, 1.7 nM; **38**, 2.4 nM) suggesting A-ring dihalogenation for this triad did not significantly impact on growth inhibition. Comparing these results to compounds containing the unnatural 2-hydroxy-4-methoxyaryl B-ring, a 5- to 20-fold loss in activity was observed for **39–41** (IC$_{50}$ values: **39**, 24.4 nM; **40**, 27.3 nM; **41**, 27.0 nM). Despite the reduction in overall activity,

1,5-geometry of the two aryl groups; an approach that has been previously used in the synthesis of closely related compounds.[12,14,19] Three azide A-ring (**17**, **22** and **27**) and three alkyne B-ring (**34–36**) coupling partners were required. These were the trimethoxy azide **17** and 3,5-dihalogenated aryl azides **22** and **27**. Azide **17** was prepared in 84% yield from **16** by treatment with sodium nitrite and displacement of the resulting diazo group using sodium azide in a one-pot procedure (Scheme 1).[24]

3,5-Dibromo aryl azide **22** was obtained in four steps from **18** in 70% overall yield via acetyl protection, phenol methylation, deacetylation and azide formation (Scheme 2).

The 3,5-diiodo aryl azide **27** was prepared via iodination[25] of **23**, phenol methylation, nitro group reduction and azide formation to give **27** in 62% overall yield (Scheme 3).

B-ring alkynes **34–36** were obtained from benzaldehydes **28–30** via *tert*-butyldimethylsilyl (TBS)-protection of the phenol groups followed by a Colvin rearrangement (Scheme 4).[26] Aldehyde **30** was produced in 86% yield from 2,3,4-methoxybenzaldehyde by selective demethylation using boron trichloride.[27] TBS-protection
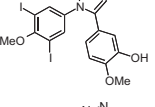

Scheme 5. Reagents and conditions: (a) EtMgCl, THF, 50 °C, 4 h; (b) TBAF, THF, rt, 1 h, 16–77% over two steps. **5** 77%, **37** 66%, **38** 53%, **39** 49%, **40** 42%, **41** 27%, **15** 35%, **42** 16%, **43** 23%.

1752

T. M. Beale et al./Bioorg. Med. Chem. 20 (2012) 1749–1759

Table 1
Activity of triazoles (**5**, **15**, **37–43**) on SK-OV-3 cells using the MTS colorimetric assay and the sulforhodamine B (SRB) assay

Cmpd.	Structure	MTS IC$_{50}$/nM[a]		SRB IC$_{50}$/nM		Cmpd	Structure	MTS IC$_{50}$/nM		SRB IC$_{50}$/nM	
		IC$_{50}$[b]	95% CI[c]	IC$_{50}$	95% CI			IC$_{50}$	95% CI	IC$_{50}$	95% CI
CA–4 (**1**)		1.7	0.9–2.5	–	–	**40**		27.4	23.9–31.0	27.3	25.6–29.0
5[d]		0.9	0.8–0.9	0.9	0.8–0.9	**41**		32.1	30.2–34.0	27.0	25.9–28.2
37		2.5	1.6–3.4	1.7	2.9–3.1	**15**[e]		17.0	14.9–19.0	17.8	16.7–18.8
38		1.9	1.4–2.4	2.4	3.3–3.4	**42**		11.6	8.0–15.2	12.8	12.2–13.5
39		29.9	25.7–34.1	24.4	23.4–25.3	**43**		32.4	30.1–34.7	30.0	28.5–31.6

[a] Concentration required to inhibit proliferation by 50%.
[b] Combined data from three separate assays were used to calculate IC$_{50}$ values.
[c] 95% confidence interval for IC$_{50}$ value.
[d] Compound first reported in Ref. 12.
[e] Compound first reported in Ref. 19.

dihalogenation of the A-ring was tolerated, since the compounds were all active at nanomolar concentrations.

Switching to the 2,3-dihydro-4-methoxyaryl B-ring (as in CA–1, **3**), resulted in an increase in the overall distribution of activity for **15**, **42–43** (IC$_{50}$ values: **15**, 17.8 nM; **42**, 12.8 nM; **43**, 30.0 nM). This activity gain presumably results from the restoration of the 3-hydroxyl group which is known to be important for binding. These IC$_{50}$ values are a significant improvement on those reported previously for the natural product CA–1 (**3**) on other cancer cell lines (IC$_{50}$ values: 0.51–13.3 μM across pancreatic, lung, prostate, neuroblastoma, thyroid and pharynx cell lines).[29] Moreover, dibrominated **42** was the most active of the triad and diiodinated **43** was only marginally less active than its unnatural congener **41**, contrary to the emerging pattern.

In summary, it would appear that dihalogenation of the A-ring in our triazole series does not affect the inherent activity of the 2- or 3-hydroxy-, or 2,3-dihydroxy B-ring substitution, and as such represents one of very few tolerated A-ring modifications in these type of compounds.

2.2.2. Cell-cycle analysis

A hallmark of antitubulin agents is their ability to arrest cycling cells in the G$_2$/M phase of the cell cycle, as we have previously shown for CA–4 (**1**) using SK-OV-3 cells.[9] To determine whether the above cytotoxic effects were due to interruption of the functioning of cellular microtubules, SK-OV-3 cells treated with **5**, **15** and **37–43** were investigated using flow cytometry. The cell cycle analyses were performed at different compound concentrations for each B-ring substitution pattern in an attempt to differentiate the

effect of A-ring substitution. Preliminary cytotoxicity assays were used to select the compound concentration used (3 nM for **5**, **37**, **38**; 12 nM for **39–41**; 15 nM for **15**, **42–43**). Unfortunately, the concentration used for compounds **39–41** was not representative of potency and therefore no antimitotic activity was observed for these compounds in this assay. The results are reported in Table 2. At a concentration of 3 nM, **5**, the direct triazole analogue of **1**, resulted in 72% of cells in G$_2$/M phase (cf 31% at 5 nM for **1**). 3,5-Dibrominated **37** was yet more effective with 88% of cells in G$_2$/M phase. 3,5-diiodinated **38** was the least active compound in this triad. The 2-hydroxyl B-ring analogues (**39–41**) did not show any

Table 2
Effect of triazoles (**5**, **15**, **37–43**) on the SK-OV-3 cell cycle

Compound	Concentration/nM	Cell cycle phase/%		
		G$_1$	S	G$_2$/M
Control	–	54	31	14
CA–4 (**1**)	5	40	23	31
5[a]	3	14	12	72
37	3	1	10	88
38	3	37	18	44
39	12	52	25	23
40	12	49	24	27
41	12	52	22	25
15[b]	15	57	24	19
42	15	4	12	84
43	15	54	25	21

[a] Compound first reported in Ref. 12.
[b] Compound first reported in Ref. 19.

Table 3
Inhibition of tubulin polymerisation for triazoles (**5**, **15**, **37–43**)

Compound	% Inhibition at 5 µM[a]
CA–4 (**1**)	57.6 ± 16.5
5[b]	101.7 ± 5.2
37	64.3 ± 11.1
38	44.8 ± 6.1
39	81.8 ± 6.2
40	12.0 ± 14.8
41	42.5 ± 16.7
15[c]	98.0 ± 3.5
42	95.7 ± 3.7
43	69.1 ± 7.3

[a] Results represent the mean of three separate experiments ± standard deviation.
[b] Compound first reported in Ref. 12.
[c] Compound first reported in Ref. 19.

appreciable increase in the percentage of cells in G_2/M phase (23–27%) over control (14%) at a concentration of **12** nM. The 2,3-dihydroxyl B-ring (CA–1) analogues (**15**, **42–43**) mirrored the results of the cytotoxicity assays. We found 3,5-dibrominated **42** to be the most effective (84%), while 3,4,5-trimethoxy **15** and 3,5-diiodinated **43** did not display any activity at a concentration of 15 nM.

Taken together, the cell cycle analysis data follow the trends observed in the growth inhibition assays. Compounds that had the lowest IC_{50} values were shown to exert the highest levels of G_2/M arrest. This suggests that the compounds are acting on the mitotic machinery of the cell and, given their structure, it is likely that this was through interaction with tubulin.

2.2.3. Inhibition of tubulin polymerisation

The effect of triazoles **5**, **15** and **37–43** and CA–4 (**1**) on tubulin polymerisation was also investigated to confirm this hypothesis. Compounds were tested at a concentration of 5 µM, and data is reported as percentage inhibition of tubulin assembly relative to control, averaged over three separate measurements (Table 3). Representative tubulin polymerisation curves are also shown (Fig. 3). These results indicate that **5**, **42** and **43** attained very high levels of tubulin polymerisation inhibition, almost completely abrogating polymerisation at a concentration of 5 µM, whereas **1** only exhibited 58% inhibition at the same concentration. Conversely, **38**, **40** and **41** had lower levels of tubulin polymerisation inhibition when compared to **1**.

Broadly, the tubulin polymerisation inhibition results map well onto the cellular data, however, the results for the diiodinated compounds **38**, **41** and **43** are noteworthy. Although **38** demonstrated high cellular potency (IC_{50} SK-OV-3; SRB 2.4 nM, MTS 1.9 nM) it did not inhibit tubulin polymerisation to the level of **1**. Compound **43** had tubulin activity greater than that of **1** but lower cellular activity (IC_{50} SK-OV-3; SRB 30.0 nM, MTS 32.4 nM). Compound **41**, that was equipotent with **43** in cells, returned a lower value for inhibition of tubulin polymerisation. Compound **43** did not follow the trend of high tubulin polymerisation observed for the other dihydroxylated compounds **15** and **42**.

2.2.4. HUVEC growth inhibition

Despite the considerable potency of the combretastatins towards cancer cells, much of the focus has been towards their use as VDAs. To investigate whether our triazole series had the potential to effect tumour vasculature, we performed growth inhibition assays using primary human umbilical vein endothelial cells (HUVECs) (Table 4). These cells were isolated from individual human umbilical cords giving genetically distinct isolates, which were assayed separately.

With the natural 3-hydroxy aryl B-ring and trimethoxyaryl A-ring, the most potent compound was **5** with an IC_{50} value (1.0 nM), exceeding that of the reference compound CA–4 (**1**, 2.2 nM). Dibrominated **37** and diiodinated **38** exhibited minor reductions in potency relative to **5** (IC_{50} values: **37**, 1.7 nM; **38**, 2.2 nM).

The unnatural 2-hydroxyl aryl B-ring compounds **39–41** were less active (IC_{50} values: **39**, 48.6 nM; **40**, 91.6 nM; **41**, 31.7 nM). Compounds containing the 2,3-dihydroxylated B-ring (as in CA–1, **3**) were active in the single digit nanomolar range (IC_{50} values: **15**, 11.8 nM; **42**, 2.3 nM, **43**, 4.3 nM).

Unexpectedly, 3,5-diiodo aryl A-ring compound **43** was found to be 7-fold more active on HUVECs than the cancer cell line (IC_{50} values: 4.3 nM cf 30 nM) (Fig. 4). This selectivity for HUVECs is a very encouraging result. Not only does it support the IC_{50} values obtained for the natural cis-stilbene CA–1 (**3**) on HUVECs in our hands (**3**, 24 h, 2.6 nM; 48 h, 4.1 nM),[30] it also indicates that the CA–1 B-ring may more generally confer selectivity for HUVECs over SK-OV-3 (ovarian) cells, as **15** and **42** are also selective for HUVECs, though to a lesser extent than **43**.

Furthermore, our results align with the reports that CA–1P (**4**) has a greater effect in preclinical models of vascular disruption
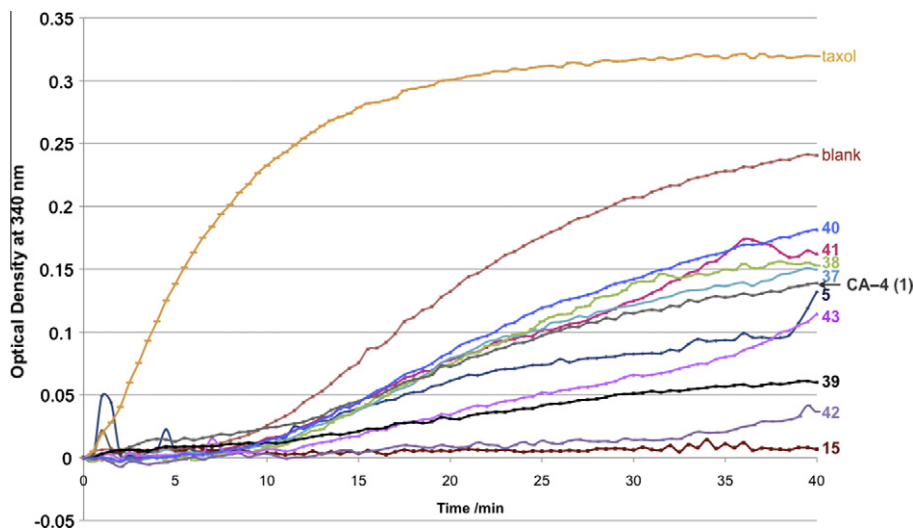

Figure 3. Representative tubulin polymerisation curves for triazoles **5**, **15**, **37–43**, CA–4 (**1**), taxol and blank.

Table 4
Activity of triazoles (**5**, **15**, **37–43**) on HUVECs using xCELLigence assay

Compound	HUVEC isolate IC$_{50}$/nM						
	1	2	3	4	5	6	Av.
CA–4 (**1**)	1.9	2.2	—	2.2	2.3	—	2.2
5[a]	0.6	0.5	2.8	0.9	0.6	0.7	1.0
37	1.1	2.2	2.2	2.5	0.6	1.5	1.7
38	1.7	5.1	1.8	3.1	0.1	1.4	2.2
39	—	—	80.4	—	36.0	29.4	48.6
40	—	—	185.9	—	42.5	46.3	91.6
41	—	11.8	54.3	—	6.1	54.7	31.7
15[b]	9.2	—	—	9.6	18.9	9.4	11.8
42	4.1	—	—	2.4	8.2	2.4	2.3
43	5.0	4.8	—	5.2	1.3	5.4	4.3

[a] Compound first reported in Ref. 12.
[b] Compound first reported in Ref. 19.

Table 5
Calculated interaction energies of triazoles (**5**, **15**, **37–43**) with tubulin (PDB:1SA0)

Compound	Total	Interaction energy/kcalmol^{-1}	
		Van der Waal's	Coulombic
5[a]	−88.30	−47.85	−40.45
37	−86.01	−47.37	−38.64
38	−90.02	−48.88	−41.14
39	−69.28	−52.93	−16.36
40[b]	−67.76	−44.93	−22.83
41	−68.71	−56.42	−12.29
15[c]	−80.11	−54.03	−26.08
42	−79.50	−51.58	−27.92
43	−81.17	−55.91	−25.26

[a] Compound first reported in Ref. 12.
[b] Binding not analogous to CA–4 (**1**).
[c] Compound first reported in Ref. 19.

than CA–4P (**2**), despite its lower growth inhibition activity on cancer cell lines in vitro.[31] However, it was shown in the same report that the unprotected 2,3-dihydroxy motif in **3** itself is chemically unstable, leading to degradation via oxidation to the *ortho*-quinone. This decomposition pathway was not noted with triazoles **15**, **42–43**.[32] The chemical stability and increased HUVEC selectivity of these 1,2,3-triazoles, especially for diiodinated **43**, suggests that they may have promise as a useful biochemical tool to better understand the mechanisms of VDAs and are worthy of further biological evaluation.

2.3. Computational studies

To gain an insight into the differences in potency observed for this set of triazoles, molecular modelling with tubulin was performed (Table 5, Fig. 5). The crystal structure of tubulin complexed to a colchicine analogue was used initially (PDB: 1SA0),[8a] with two short missing loops built and subsequently refined using the DOPE module in the Modeller suite.[33] This system, containing dimeric tubulin, Mg^{2+}-complexed GDP and GTP, was used to dock the triazole compounds **5**, **15** and **37–43** in place of colchicine in a variety of orientations. The entire protein-ligand complex was subsequently optimized via repeated rounds of thousand-step steepest descent and adopted basis Newton-Raphson minimizations with CHARMM,[34] using the CHARMM27/CMAP[35] and CHARMM general[36] force fields.

All compounds were consistently predicted to bind analogously to CA–4 (**1**) and colchicine, with the 4-methoxy on the A-ring prox-
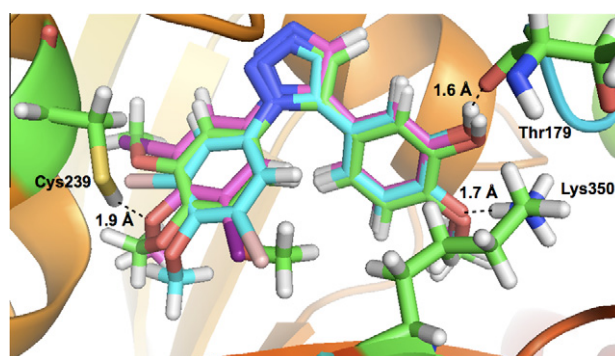

Figure 5. Modelled binding to tubulin for **5** (green), **37** (cyan) and **38** (magenta) showing key interactions and distances.

imal to Cys239, with the exception of dibrominated 2-hydroxy triazole **40**. The calculated interaction energies have a greater than 85% correlation with the experimental values obtained on the SK-OV-3 cell line.

The 3-hydroxylated compounds (**5**, **37**, **38**) all maintain the same protein interactions with their B-ring; the 3-hydroxy group forms a hydrogen bond with the backbone carbonyl of Thr179 and the 4-methoxy group interacts with the sidechain of Lys350 through oxygen in all cases. This is slightly different than the previously reported interactions for compound **5**, in which the 3-hy-
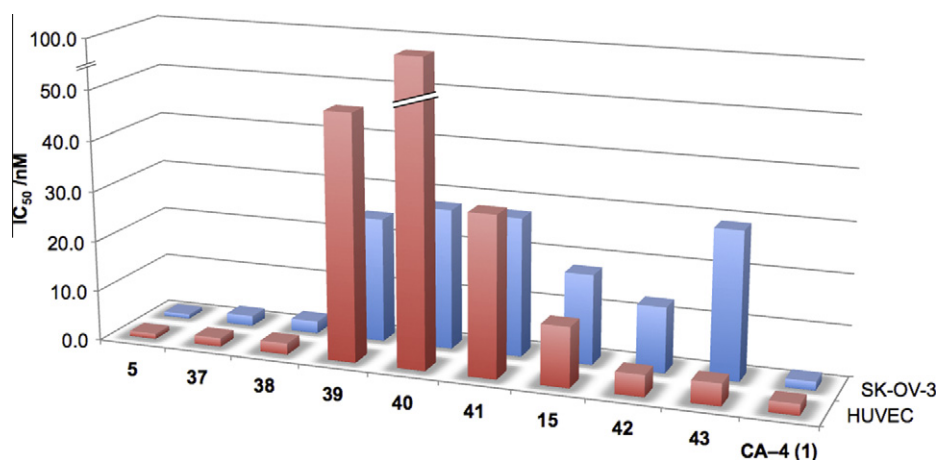

Figure 4. Comparison of growth inhibition activity of triazoles **5**, **15**, **37–44** and CA–4 (**1**) on SK-OV-3 and HUVEC cells.
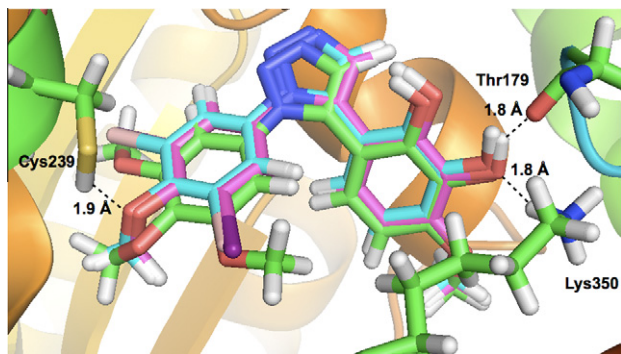
Figure 6. Modelled binding to tubulin for **15** (green), **42** (cyan) and **43** (magenta) showing key interactions and distances.

droxy group interacts with Val181 through oxygen, and the 4-methoxy group is not reported to interact directly with the protein.[8] There is flexibility in the position of the A-ring; trimethoxyaryl **5** and diiodinated **38** maintain hydrogen bonds with Cys239, whereas this contact is not present for dibrominated **37**. This loss in Coulombic interaction results in a lower overall interaction energy for **37** and may offer a reason for its lower cellular potency relative to **5** and **38**.

Movement of the hydroxyl to the 2-position on the B-ring results in a loss of interaction with Thr179, which is seen for compounds **39–41**. This explains the much lower interaction energies observed for these analogues, which is consistent with the biological assay results. Compounds **39** and **41** remain in a similar binding mode to the 3-hydroxylated compounds, whereas the lowest energy conformation attained by **40** is opposite to the other triazoles; the B-ring is nearer Cys239, but displaced so that the 2-hydroxy is hydrogen-bonded to the backbone carbonyl of Val236, though this confirmation is very close in energy to the conformation analogous to the other 2-hydroxylated compounds (Fig. S1, Supplementary data).

Dihydroxylated compounds **15**, **42–43** have greater interaction energies than their 2-hydroxylated congeners (**39–41**) but still less than the 3-hydroxylated analogues (**5**, **37**, **38**). This is due to re-establishment of the 3-hydroxy to Thr179 hydrogen bond resulting in an energy gain (Fig. 6). However, the Lys350 side-chain now interacts with the 3-hydroxyl oxygen rather than the 4-methoxy oxygen (seen for **5**, **37** and **38**) resulting in a slight loss in energy. This geometry of compounds in the colchicine-binding site is close to that previously reported for **15**, although the binding of the B-ring methoxy and hydroxyl groups was not described in detail.[19]

In summary, the molecular modelling has predicted that all but one triazole binds analogously to CA–4 (**1**) in the colchicine binding site of tubulin, and offers an explanation for the differences in activity when the B-ring is altered. It also shows that dihalogenation of the A-ring does not have a large effect on the predicted interaction energies for a fixed B-ring substitution pattern, although there is some flexibility in A-ring position within the colchicine site.

3. Conclusions

In this work, we have synthesised nine triazole-containing combretastatin analogues, varying both A-ring and B-ring substitution. These compounds maintain nanomolar activity against ovarian cancer cells and endothelial cells, and were shown to inhibit tubulin polymerisation and arrest cells in the G_2/M phase of the cell cycle. A-ring 3,5-dihalogenation was shown to be a tolerated modification, with B-ring substitution responsible for much of the differences in activity between these compounds. Computa-

tional modelling reinforced the rationale for the observed activity profiles, and generally a CA–4 (**1**) binding mode was observed.

Although **5**, the direct triazole analogue of CA–4 (**1**), was the most potent compound across the assays used to characterise the activity of these compounds, the most interesting compound of this series was the 3,5-diiodinated compound **43**, which possesses the B-ring motif found in CA–1 (**3**). This is due to its high (7-fold) selectivity for HUVECs over the ovarian cancer cell line SK-OV-3. This selectivity for the vascular cell type, coupled with chemical stability not usually associated with the dihydroxy-motif in combretastatin analogues,[29] renders this compound particularly attractive for further biological investigation as an anti-vascular agent.

4. Experimental section

Anhydrous reactions were run in oven-dried glassware under an inert atmosphere. Solvents were purified and dried using standard methods as required. Commercially available reagents were used as supplied or purified using standard procedures. Microwave reactions were performed using a Biotage Initiator. Flash chromatographic purifications were performed under pressure on columns packed with Merck silica gel 60, particle size 40–63 nm. Hexanes refers to petroleum ether distillate (bp 40–60 °C). Analytical TLC was carried out using silica gel 60 F_{254} pre-coated glass backed plates. ^{1}H NMR and ^{13}C NMR spectra were recorded on a Bruker DPX-400 (400 MHz) spectrometer unless otherwise stated. Chemical shifts are reported in ppm with the solvent resonance resulting from incomplete deuteration as the internal standard. For ^{1}H NMR: $CDCl_3$ 7.26 ppm, CD_3OD 3.31 ppm. For ^{13}C NMR: [13]$CDCl_3$ 77.0 ppm, t;. [13]CD_3OD 49.0 ppm, heptuplet. Infrared spectra were recorded as thin films on a Perkin–Elmer Spectrum One FT-IR spectrometer and selected absorbances only are reported. High resolution mass spectrometry (HRMS) was performed on a Waters Micromass LCT spectrometer using electrospray ionisation and Micromass MS software.

Dimethyl sulfoxide (DMSO), RPMI-1640, propidium iodide, RNase A, trichloroacetic acid and sulforhodamine B were purchased from Sigma, UK. Trypsin/EDTA solution, Endothelial Basal Medium-2 and Single Quot® Kit supplements (EGM-2) were purchased form Lonza Group Ltd., UK. The CellTiter 96® Aqueous One Solution Reagent was purchased from Promega, UK. Tubulin (>99% pure), PIPES, EGTA, magnesium chloride, GTP, glycerol and taxol were purchased as part of the tubulin polymerization assay kit from Cytoskeleton, Inc., USA. SK-OV-3 cells were grown from stocks held in the Cancer Research UK Cambridge Research Institute (CRI). Human umbilical vein endothelial cells (HUVECs) were isolated from umbilical cords following elective caesarean sections performed in the Rosie Hospital, Addenbrookes, Cambridge. This study was approved by the Local Research Ethics Committee and all patients gave written informed consent. Cancer cells were sub-cultured as previously described.[9] HUVECs were isolated, cultured, stored and their purity determined as previously described.[9] All isolates used in this work were >99.5% pure as determined by immunocytochemistry using anti-fibroblast, anti smooth muscle actin and anti-CD31 antibodies.

4.1. General procedure for azide formation

$NaNO_2$ (2.28 mmol) in H_2O (5 mL) was added dropwise to a slurry of aniline (1.90 mmol) in H_2O/HCl (1:1, 20 mL) at 0 °C then stirred for 1 h. A solution of NaN_3 (2.28 mmol) in H_2O (5 mL) was then added dropwise and the resulting suspension was allowed to warm to rt over 2 h. The mixture was diluted with EtOAc (20 mL) and the aqueous layer was extracted further with EtOAc (2 × 20 mL). The combined organic phases were washed with brine (20 mL), dried over $MgSO_4$ and concentrated in vacuo.

4.2. General procedure for phenol protection

A solution of TBSCl (36.00 mmol) in DMF (20 mL) was added dropwise to a solution of Et₃N (40.00 mmol) and hydroxybenzaldehyde (33.00 mmol) in DMF (10 mL) then stirred for 18 h at rt. The reaction was diluted with H₂O (100 mL) then extracted with EtOAc (3 × 100 mL) and the combined organic phases were washed with 10% aq. LiCl (100 mL), H₂O (100 mL), and brine (50 mL), dried over MgSO₄ and concentrated in vacuo. The residue was purified by flash column chromatography (0–15% EtOAc in hexanes).

4.3. General procedure for Colvin rearrangement

2.0 M TMS-diazomethane in hexanes (2.47 mL) was added dropwise to a solution of 0.1 M LDA in THF (6.20 mL) at −78 °C and the reaction was stirred for 1 h. A solution of benzaldehyde (4.43 mmol) in THF (15 mL) at −78 °C was then added via cannula. After a further 1 h stirring at −78 °C the reaction was allowed to warm to rt and stirred for a further 1 h. the reaction was then diluted with brine (20 mL) and EtOAc (30 mL) and the organic layer was separated and the aqueous layer was extracted with EtOAc (2 × 30 mL). The combined organic phases were dried over MgSO₄ and concentrated in vacuo. The residue was purified by flash column chromatography (0–20% EtOAc in hexanes).

4.4. General procedure for Huisgen cycloaddition

A solution of alkyne (0.19 mmol) in THF (0.5 mL) was added dropwise to a solution of EtMgCl (136 µL of 1.40 M in THF) in THF (2.5 mL) at rt. The solution was heated to 50 °C for 30 min, then allowed to cool to rt before the dropwise addition of a solution of azide (0.19 mmol) in THF (1.0 mL). The solution was heated again to 50 °C for 3 h then diluted with saturated aq. NH₄Cl (5 mL) and CH₂Cl₂ (10 mL). The organic layer was separated and the aqueous layer was extracted with CH₂Cl₂ (2 × 10 mL). The combined organic phases were washed with brine (10 mL), dried over MgSO₄ and concentrated in vacuo. The residue was purified by flash column chromatography (5–15% EtOAc in hexanes).

4.5. General procedure for silyl group deprotection

TBAF (410 µL of 1 M solution in THF) was added dropwise to a solution of silyl-protected triazole (0.28 mmol) in THF (5 mL) at 0 °C. The reaction was allowed to warm to rt and stirred for 1 h. Ice (2 mL), H₂O (2 mL) and EtOAc (10 mL) were then added and the mixture stirred for 5 min. The organic layer was separated and the aqueous layer extracted with EtOAc (2 × 10 mL). The combined organic phases were washed with brine (10 mL), dried over MgSO₄ and concentrated in vacuo. The residue was purified by flash column chromatography (40–60% EtOAc in hexanes).

4.6. 5-Azido-1,2,3-trimethoxybenzene (17)[37]

Prepared from aniline **16** (2.00 g, 10.90 mmol) using the general procedure for azide formation to give **17** (1.92 g, 9.2 mmol, 84%) as a red oil. R_f 0.51 (30% EtOAc in hexanes); ¹H NMR (CDCl₃): δ 3.82 (s, 3H), 3.86 (s, 6H), 6.25 (s, 2H); ¹³C NMR (CDCl₃): δ 56.2, 61.0, 96.6, 135.7, 148.6, 154.1; IR (ATR) v/cm⁻¹ 2942, 2101, 1585, 1504.

4.7. 5-Azido-1,3-dibromo-2-methoxybenzene (22)

Prepared from aniline **21** (1.00 g, 3.56 mmol) using the general procedure for azide formation to give **22** (994 mg, 3.23 mmol, 91%) as a red solid. R_f 0.75 (30% EtOAc in hexanes); ¹H NMR (CDCl₃): δ 3.87 (s, 3H), 7.18 (s, 2H); ¹³C NMR (CDCl₃): δ 60.9, 118.9, 123.0, 137.7, 151.5; IR (ATR) v/cm⁻¹ 2955, 2109, 1587, 1546. HRMS-EI m/z [M+H]⁺ calcd for C₇H₅N₃OBr₂: 304.8794, found: 304.8801.

4.8. 5-Azido-1,3-diiodo-2-methoxybenzene (27)

Prepared from aniline **26** (713 mg, 1.90 mmol) using the general procedure for azide formation to give **27** (728 mg, 1.82 mmol, 96%) as a brown solid. R_f 0.70 (20% EtOAc in hexanes); ¹H NMR (CDCl₃): δ 3.83 (s, 1H), 7.40 (s, 1H); ¹³C NMR (CDCl₃): δ 61.0, 90.6, 130.0, 138.2, 156.4; IR (ATR) v/cm⁻¹ 2940, 2109, 1575, 1534. HRMS-EI m/z [M+H]⁺ calcd for C₇H₅N₃OI₂: 400.8517, found: 400.8516.

4.9. 3-((*tert*-Butyldimethylsilyl)oxy)-4-methoxybenzaldehyde (31)[38]

Prepared from aldehyde **28** (5.00 g, 32.86 mmol) using the general procedure for phenol protection to give **31** (8.74 g, 32.81 mmol, quant.) as a pale yellow oil. R_f 0.71 (40% EtOAc in hexanes); ¹H NMR (CDCl₃): δ 0.17 (s, 6H), 1.00 (s, 9H), 3.89 (s, 3H), 6.95 (d, J = 8.3 Hz, 1H), 7.36 (d, J = 2.0 Hz, 1H), 7.47 (dd, J = 8.3, 2.0 Hz, 1H), 9.82 (s, 1H); ¹³C NMR (CDCl₃): δ −4.6, 18.5, 25.7, 55.6, 111.2, 120.1, 126.2, 130.3, 145.6, 156.6, 190.9; IR (ATR) v/cm⁻¹ 2930, 2858, 1689; HRMS-ESI m/z [M+H]⁺ calcd for C₁₄H₂₃O₃Si: 267.1416, found: 267.1424.

4.10. 2-((*tert*-Butyldimethylsilyl)oxy)-4-methoxybenzaldehyde (32)[39]

Prepared from aldehyde **29** (5.00 g, 32.86 mmol) using the general procedure to give **32** (5.93 g, 22.26 mmol, 68%) as a pale yellow oil. R_f 0.69 (60% EtOAc in hexanes); ¹H NMR (CDCl₃): δ 0.29 (s, 6H), 1.03 (s, 9H), 3.84 (s, 3H), 6.35 (d, J = 2.3 Hz, 1H), 6.59 (ddd, J = 8.8, 2.3, 0.8 Hz, 1H), 7.79 (d, J = 8.8 Hz, 1H), 10.30 (d, J = 0.8 Hz, 1H); ¹³C NMR (CDCl₃): δ −4.3, 18.4, 25.7, 55.5, 105.3, 107.9, 121.5, 130.2, 160.7, 165.8, 188.6; IR (ATR) v/cm⁻¹ 2956, 2932, 2859, 1682; HRMS-ESI m/z [M+H]⁺ calcd for C₁₄H₂₃O₃Si: 267.1416, found: 267.1428.

4.11. 2,3-bis((*tert*-Butyldimethylsilyl)oxy)-4-methoxybenzaldehyde (33)[3b]

BCl₃ (17.5 mL of 1 M solution in CH₂Cl₂) was added dropwise to a solution of 2,3,4-trimethoxybenzaldehyde (3.43 g, 17.5 mmol) in CH₂Cl₂ (35 mL). Solution stirred for 2 h at rt. BCl₃ (17.5 mL of 1 M solution in CH₂Cl₂) was added dropwise and the solution was stirred for 18 h at rt. Saturated aqueous NaHCO₃ (300 mL) was added, then 3 M aqueous HCl (300 mL). The organic layer was separated and the aqueous layer extracted with EtOAc (3 × 200 mL). The combined organic phases were washed with brine (200 mL), dried over MgSO₄ and concentrated in vacuo. The residue was purified by flash column chromatography (50% EtOAc in hexanes) to give **30** as colourless crystals (2.54 g, 15.1 mmol, 86%). TBSCl (1.06 g, 7.01 mmol) in DMF (10 mL) was added dropwise to a solution of **30** (393 mg, 2.34 mmol) in DMF (10 mL) containing Et₃N (988 µL, 7.48 mmol). DMAP (57 mg, 0.47 mmol) was added in one portion and the solution was stirred for 18 h at rt. The reaction was diluted with H₂O (20 mL) and the solution extracted with EtOAc (3 × 30 mL). The combined organic phases were washed with 10% aq. LiCl (40 mL), H₂O (40 mL) and brine (30 mL), dried over MgSO₄ and concentrated in vacuo. The residue was purified by flash column chromatography (1% EtOAc in hexanes) to give **33** (887 mg, 2.24 mmol, 96%) as a white solid. R_f 0.67 (30% EtOAc in hexanes); ¹H NMR (CDCl₃): δ 0.14 (s, 12H), 1.00 (s, 9H), 1.05 (s, 9H), 3.84 (s, 3H), 6.63 (d, J = 8.8 Hz, 1H), 7.49 (d, J = 8.8 Hz, 1H), 10.23 (s, 1H); ¹³C NMR (CDCl₃): δ -3.783, -3.778, 18.6, 18.8, 26.1,

26.2, 55.2, 105.5, 121.4, 123.4, 136.9, 151.0, 157.5, 189.2; IR (ATR) v/cm^{-1} 2929, 2859, 1679; HRMS-ESI m/z [M+H]$^+$ calcd for $C_{20}H_{37}O_4Si_2$: 397.2230, found: 397.2247.

4.12. *tert*-Butyl(5-ethynyl-2-methoxyphenoxy)dimethylsilane (34)[12]

Prepared from benzaldehyde **31** (1.18 g, 4.43 mmol) using the general procedure for the Colvin rearrangement to give **34** (858 mg, 3.27 mmol, 74%) as a colourless oil. R_f 0.70 (20% EtOAc in hexanes); ^{1}H NMR (CDCl$_3$): δ 0.15 (s, 6H), 1.00 (s, 9H), 2.96 (s, 1H), 3.81 (s, 3H), 6.77 (d, J = 8.3 Hz, 1H), 6.98 (d, J = 2.0 Hz, 1H), 7.09 (dd, J = 8.3, 2.0 Hz, 1H); ^{13}C NMR (CDCl$_3$): δ -4.6, 18.5, 25.7, 55.4, 75.5, 83.8, 111.7, 114.2, 124.5, 126.4, 144.7, 152.1; IR (ATR) v/cm^{-1} 3314, 2930, 2859, 1573; HRMS-ESI m/z [M+H]$^+$ calcd for $C_{15}H_{23}O_2Si$: 263.1467, found: 263.1477.

4.13. *tert*-Butyl(2-ethynyl-5-methoxyphenoxy)dimethylsilane (35)

Prepared from benzaldehyde **32** (0.50 g, 1.88 mmol) using the general procedure for the Colvin rearrangement to give **35** (256 mg, 0.98 mmol, 52%) as a pale yellow oil. R_f 0.73 (30% EtOAc in hexanes); ^{1}H NMR (CDCl$_3$): δ 0.24 (s, 6H), 1.03 (s, 9H), 3.10 (s, 1H), 3.78 (s, 3H), 6.37 (d, J = 2.5 Hz, 1H), 6.48 (dd, J = 8.6, 2.5 Hz, 1H), 7.33 (d, J = 8.6 Hz, 1H); ^{13}C NMR (CDCl$_3$): δ -4.2, 18.3, 25.8, 55.3, 79.5, 81.1, 106.1, 106.9, 107.3, 134.6, 158.4, 161.0; IR (ATR) v/cm^{-1} 3315, 2930, 2859, 2106, 1605; HRMS-ESI m/z [M+H]$^+$ calcd for $C_{15}H_{23}O_2Si$: 263.1467, found: 263.1458.

4.14. ((3-Ethynyl-6-methoxy-1,2-phenylene)bis(oxy))bis(*tert*-butyldimethylsilane) (36)

Prepared from **33** (816 mg, 2.06 mmol) using the general procedure for the Colvin rearrangement to give **36** (517 mg, 1.32 mmol, 64%) as a colourless oil. R_f 0.73 (10% EtOAc in hexanes); ^{1}H NMR (CDCl$_3$): δ 0.11 (s, 6H), 0.20 (s, 6H), 1.00 (s, 9H), 1.05 (s, 9H), 3.08 (s, 1H), 3.77 (s, 3H), 6.46 (d, J = 8.6 Hz), 7.02 (d, J = 8.6 Hz, 1H); ^{13}C NMR (CDCl$_3$): δ -3.8, -3.3, 18.5, 18.8, 26.1, 26.4, 55.0, 79.8, 82.2, 104.9, 109.2, 126.4, 137.1, 149.3, 153.3; IR (ATR) v/cm^{-1} 3314, 2930, 2858, 2106, 1592; HRMS-ESI m/z [M+H]$^+$ calcd for $C_{21}H_{37}O_3Si_2$: 393.2281, found: 393.2299.

4.15. 2-Methoxy-5-(1-(3,4,5-trimethoxyphenyl)-*1H*-1,2,3-triazol-5-yl)phenol (5)[12]

Prepared from azide **17** (100 mg, 0.38 mmol) and alkyne **34** (80 mg, 0.38 mmol) using the general procedure for the Huisgen cycloaddition to give TBS-protected **5** (137 mg, 0.29 mmol, 77%) as a yellow oil. **5** was obtained after silyl deprotection using the general procedure (104 mg, 0.28 mmol, quant.) as a white solid. R_f 0.12 (50% EtOAc in hexanes); ^{1}H NMR (CDCl$_3$): δ 3.74 (s, 6H), 3.88 (s, 3H), 3.91 (s, 3H), 5.78 (s, 1H), 6.60 (s, 2H), 6.73 (dd, J = 8.4, 2.1 Hz, 1H), 6.82 (d, J = 8.4 Hz, 1H) 6.88 (d, J = 2.1 Hz, 1H), 7.78 (s, 1H); ^{13}C NMR (CDCl$_3$): δ 56.1, 56.3, 61.1, 103.0, 110.8, 114.9, 119.9, 120.8, 132.2, 133.1, 137.5, 138.7, 145.9, 147.4, 153.5; IR (ATR) v/cm^{-1} 2939, 2838, 1599, 1506, 1464, 1417, 1228, 1125, 1022, 995, 811, 730; HRMS-ESI m/z [M+H]$^+$ calcd for $C_{18}H_{20}N_3O_5$: 358.1403, found: 358.1400.

4.16. 5-(1-(3,5-Dibromo-4-methoxyphenyl)-*1H*-1,2,3-triazol-5-yl)-2-methoxyphenol (37)

Prepared from azide **22** (100 mg, 0.38 mmol) and alkyne **34** (117 mg, 0.38 mmol) using the general Huisgen cycloaddition procedure described above to give TBS-protected **37** (149 mg,

0.26 mmol, 69%) as an orange oil. **37** was obtained after silyl deprotection using the general procedure (91 mg, 0.20 mmol, 95%) as a white solid. R_f 0.26 (50% EtOAc in hexanes); ^{1}H NMR (CDCl$_3$): δ 3.92 (s, 3H), 3.93 (s, 3H), 6.71 (dd, J = 8.4, 2.2 Hz, 1H), 6.84 (d, J = 2.2 Hz, 1H), 6.85 (d, J = 8.4 Hz, 1H), 7.56 (s, 2H), 7.75 (s, 1H). ^{13}C NMR (CDCl$_3$): δ 56.1, 60.9, 111.1, 114.8, 118.5, 118.9, 120.9, 129.2, 133.3, 133.8, 137.8, 146.2, 147.9, 155.0; IR (ATR) v/cm^{-1} 3080, 2937, 2840, 1619, 1583; HRMS-ESI m/z [M+H]$^+$ calcd for $C_{16}H_{14}N_3O_3Br_2$: 453.9402, found: 453.9419.

4.17. 5-(1-(3,5-Diiodo-4-methoxyphenyl)-*1H*-1,2,3-triazol-5-yl)-2-methoxyphenol (38)

Prepared from azide **27** (76 mg, 0.19 mmol) and alkyne **34** (50 mg, 0.19 mmol) using the general Huisgen cycloaddition procedure described above to give TBS-protected **38** (105 mg, 0.16 mmol, 83%) as a pale yellow solid. **38** was obtained after silyl deprotection using the general procedure (52 mg, 0.09 mmol, 50%) as a white solid. R_f 0.20 (40% EtOAc in hexanes); ^{1}H NMR (CDCl$_3$): δ 3.91 (s, 3H), 3.94 (s, 3H), 5.76 (s, 1H), 6.71 (dd, J = 8.3, 2.2 Hz, 1H), 6.84 (d, J = 2.2 Hz, 1H), 6.86 (d, J = 8.3 Hz, 1H), 7.76 (s, 1H), 7.80 (s, 2H); ^{13}C NMR (CDCl$_3$): δ 56.1, 60.9, 90.0, 111.0, 114.7, 119.0, 120.9, 133.2, 134.4, 136.1, 137.7, 146.1, 147.7, 159.8; IR (ATR) v/cm^{-1} 3007, 1619, 1579; HRMS-ESI m/z [M+H]$^+$ calcd for $C_{16}H_{14}N_3O_3I_2$: 549.9125, found: 549.9117.

4.18. 5-Methoxy-2-(1-(3,4,5-trimethoxyphenyl)-*1H*-1,2,3-triazol-5-yl)phenol (39)

Prepared from azide **17** (200 mg, 0.76 mmol) and alkyne **35** (145 mg, 0.69 mmol) using the general Huisgen cycloaddition procedure described above to give TBS-protected **39** (158 mg, 0.34 mmol, 49%) as a yellow oil. **39** was obtained after silyl deprotection using the general procedure (101 mg, 0.28 mmol, quant.) as a pale pink solid. R_f 0.12 (30% EtOAc in hexanes); ^{1}H NMR (CDCl$_3$): δ 3.67 (s, 6H), 3.78 (s, 3H), 3.81 (s, 3H), 6.43 (dd, J = 8.6, 2.5 Hz, 1H), 6.66 (partially obscured d, 1H), 6.67 (s, 2H), 6.93 (d, J = 8.6 Hz, 1H), 7.76 (s, 1H); ^{13}C NMR (CDCl$_3$): δ 55.4, 56.2, 61.0, 102.0, 102.6, 106.4, 106.5, 131.6, 132.6, 134.1, 134.7, 138.1, 153.2, 156.4, 162.2; IR (ATR) v/cm^{-1} 3118, 2941, 2837, 1622, 1600; HRMS-ESI m/z [M+H]$^+$ calcd for $C_{18}H_{20}N_3O_5$: 358.1403, found: 358.1396.

4.19. 2-(1-(3,5-Dibromo-4-methoxyphenyl)-*1H*-1,2,3-triazol-5-yl)-5-methoxyphenol (40)

Prepared from azide **22** (56 mg, 0.21 mmol) and alkyne **35** (64 mg, 0.21 mmol) using the general Huisgen cycloaddition procedure described above to give TBS-protected **40** (77 mg, 0.14 mmol, 64%) as an orange oil. Compound **40** was obtained after silyl deprotection using the general procedure (39 mg, 0.09 mmol, 66%) as a pale brown solid. R_f 0.15 (30% EtOAc in hexanes); ^{1}H NMR (500 MHz, CD$_3$OD): δ 3.79 (s, 3H), 3.89 (s, 3H), 6.40 (d, J = 2.4 Hz, 1H), 6.53 (dd, J = 8.5, 2.4 Hz, 1H), 7.13 (d, J = 8.5 Hz, 1H), 7.64 (s, 2H), 7.80 (s, 1H); ^{13}C NMR (125 MHz, CD$_3$OD): δ 55.8, 61.3, 102.5, 106.8, 106.9, 118.9, 129.5, 132.9, 134.9, 136.2, 137.5, 156.0, 157.5, 164.2; IR (ATR) v/cm^{-1} 2925, 1618, 1587; HRMS-ESI m/z [M+H]$^+$ calcd for $C_{16}H_{14}N_3O_3Br_2$: 453.9402, found: 453.9422.

4.20. 2-(1-(3,5-Diiodo-4-methoxyphenyl)-*1H*-1,2,3-triazol-5-yl)-5-methoxyphenol (41)

Prepared from **27** (76 mg, 0.19 mmol) and **35** (50 mg, 0.19 mmol) using the general Huisgen cycloaddition procedure described above to give TBS-protected **41** (43 mg, 0.07 mmol, 34%) as a pale yellow solid. Compound **41** was obtained after silyl

deprotection using the general procedure (25 mg, 0.05 mmol, 80%) as a white solid. R_f 0.37 (50% EtOAc in hexanes); ^{1}H NMR (500 MHz, CD$_3$OD): δ 3.77 (s, 3H), 3.83 (s, 3H), 6.39 (d, J = 2.3 Hz, 1H), 6.51 (dd, J = 8.5, 2.3 Hz, 1H), 7.09 (d, J = 8.5 Hz, 1H), 7.77 (s, 1H), 7.82 (s, 2H); ^{13}C NMR (125 MHz, CD$_3$OD): δ 55.8, 61.3, 90.3, 102.5, 106.8, 106.9, 132.9, 134.8, 136.36, 136.44, 137.4, 157.6, 161.1, 164.2; IR (ATR) v/cm^{-1} 3075, 2926, 1620, 1579; HRMS-ESI m/z [M+H]$^+$ calcd for C$_{16}$H$_{14}$N$_3$O$_3$I$_2$: 549.9125, found: 549.9145.

4.21. 3-Methoxy-6-(1-(3,4,5-trimethoxyphenyl)-*1H*-1,2,3-triazol-5-yl)benzene-1,2-diol (15)[19]

Prepared from azide **17** (27 mg, 0.13 mmol) and alkyne **36** (52 mg, 0.13 mmol) using the general Huisgen cycloaddition procedure described above to give TBS-protected **42** (42 mg, 0.07 mmol, 54%) as a pale yellow oil. Compound **42** was obtained after silyl deprotection using the general procedure (15 mg, 0.04 mmol, 64%) as a white solid. R_f 0.12 (30% EtOAc in hexanes); ^{1}H NMR (CDCl$_3$): δ 3.72 (s, 6H), 3.86 (s, 3H), 3.90 (s, 3H), 5.56 (s, 1H), 5.63 (s, 1H), 6.47 (d, J = 8.6 Hz, 1H), 6.62 (d, J = 8.6 Hz, 1H), 6.65 (s, 2H), 7.87 (s, 1H); ^{13}C NMR (125 MHz, CDCl$_3$): δ 56.17, 56.23, 61.0, 102.0, 103.1, 107.6, 121.4, 132.6, 132.8, 133.6, 134.6, 138.1, 142.3, 147.8, 153.2; IR (ATR) v/cm^{-1} 3675, 2971, 1628, 1604; HRMS-ESI m/z [M+H]$^+$ calcd for C$_{18}$H$_{20}$N$_3$O$_6$: 374.1352, found: 374.1345.

4.22. 3-(1-(3,5-Dibromo-4-methoxyphenyl)-*1H*-1,2,3-triazol-5-yl)-6-methoxybenzene-1,2-diol (42)

Prepared from azide **22** (61 mg, 0.16 mmol) and alkyne **36** (48 mg, 0.16 mmol) using the general Huisgen cycloaddition procedure described above to give TBS-protected **43** (33 mg, 0.05 mmol, 30%) as a pale yellow oil. Compound **43** was obtained after silyl deprotection using the general procedure (12 mg, 0.03 mmol, 52%) as a white solid. R_f 0.14 (70% EtOAc in hexanes); ^{1}H NMR (CDCl$_3$): δ 3.91 (s, 3H), 3.93 (s, 3H), 5.57 (br s, 2H), 6.52 (d, J = 8.6 Hz, 1H), 6.65 (d, J = 8.6 Hz, 1H), 7.60 (s, 2H), 7.82 (s, 1H); ^{13}C NMR (CDCl$_3$): δ 56.3, 60.8, 90.0, 103.4, 106.7, 118.1, 121.4, 128.4, 132.8, 134.7, 140.2, 142.0, 148.2, 162.9; IR (ATR) v/cm^{-1} 2923, 2853, 1703, 1590; HRMS-ESI m/z [M+H]$^+$ calcd for C$_{16}$H$_{14}$N$_3$O$_4$Br$_2$: 469.9351, found: 469.9348.

4.23. 3-(1-(3,5-Diiodo-4-methoxyphenyl)-*1H*-1,2,3-triazol-5-yl)-6-methoxybenzene-1,2-diol (43)

Prepared from **27** (99 mg, 0.25 mmol) and **36** (100 mg, 0.25 mmol) using the general Huisgen cycloaddition procedure described above to give TBS-protected **44** (75 mg, 0.10 mmol, 38%) as a pale yellow oil. Compound **44** was obtained after silyl deprotection using the general procedure (32 mg, 0.06 mmol, 60%) as a white solid. R_f 0.31 (60% EtOAc/Petrol). ^{1}H NMR (CD$_3$OD): δ 3.85 (s, 3H), 3.88 (s, 3H), 6.59 (d, J = 8.6 Hz, 1H), 6.64 (d, J = 8.6 Hz, 1H), 7.79 (s, 1H), 7.83 (s, 2H). ^{13}C NMR (125 MHz, CD$_3$OD): δ 56.6, 61.3, 90.4, 104.5, 107.9, 121.7, 134.9, 135.7, 136.3, 136.4, 137.4, 138.7, 145.2, 151.3, 161.1; IR (ATR) v/cm^{-1} 3483, 3008, 2927, 1633, 1578; HRMS-ESI m/z [M+H]$^+$ calculated for C$_{16}$H$_{14}$N$_3$O$_4$I$_2$: 565.9074, found: 565.9085.

4.24. MTS Assay

SK-OV-3 cells were seeded at 8.0×10^3 cells per well in RPMI-1640 medium (180 μL) and incubated for 24 h, before addition of drug compound in medium (20 μL, 10× concentrations to give appropriate 1 × plate concentrations). Plates were incubated for 48 h, and the media was then aspirated. CellTiter 96® AQueous One Solution Reagent (20 μL) in fresh media (100 μL) was added to each well. Plates were incubated excluding light for 2 h, and absorbance at 492 nm was measured. IC$_{50}$ and CI values were calculated using a 4-parameter log-linear dose-response curve using the DRC package[40] in R.[41]

4.25. SRB Assay

SK-OV-3 cells were seeded at 8.0×10^3 cells per well in RPMI-1640 medium (180 μL), and incubated for 24 h, before addition of drug compound in medium (20 μL, 10× concentrations to give appropriate 1 × plate concentrations). Plates were incubated for 48 h, and the media was then aspirated. Cells fixed for 1 h at 0 °C with 3% (v/v) trichloroacetic acid in water (100 μL), then stained with 0.4% SRB in 1% acetic acid (100 μL) for 30 min, washed with 1% acetic acid (4 × 200 μL) and solubilised with 10 mM Tris base (100 μL) for 30 min. Absorbance was measured at 570 nm. IC$_{50}$ and CI values were calculated using a 4-parameter log-linear dose-response curve using the DRC[39] package in R.[40]

4.26. Tubulin assay

Purified bovine tubulin (>99% pure, 3 mg/ml) in 80 mM PIPES pH 7.0, 0.5 mM EGTA, 2 mM MgCl$_2$, 1 mM GTP and 10% glycerol (90 μL) was added to each well of a pre-warmed 96-well plate at 37 °C containing 10× drug solution in 80 mM PIPES pH 7.0, 0.5 mM EGTA, 2 mM MgCl$_2$ (10 μL). The effect on tubulin assembly was monitored in a PHERAstar FS spectrophotometer at 340 nm at 30 s intervals for 60 min at 37 °C. Percentage inhibition of polymerization was recorded for each reaction. The results represent the mean of three separate experiments ± standard deviation.

4.27. xCELLigence assay

HUVECs were seeded at 7.5×10^3 cells per well in EGM-2 (90 μL) into an E-plate 96 after determination of background impedance then incubated for 5 h in the Real-Time Cell Analyzer (RTCA) station, recording impedance every 10 min. Drug compound was then added in EGM-2 (10 μL, 10 × concentrations to give appropriate 1× plate concentrations) and the plate returned to the RTCA. Impedance was recorded every 40 s for 3 h, then every 30 min for 21 h. Dose–response curves were generated and used to determine IC$_{50}$ values using a 4-parameter log-linear dose–response curve.

4.28. Computational studies

Each system contained dimeric tubulin, Mg^{2+}-complexed GDP and GTP, and the docked triazole compound. All ionisable groups of the protein were assigned their most probable charged states at neutral pH. Two missing short loops in the protein were built using the Modeller suite, initially using the "loop-model" module to generate 1000 models, and subsequently refining the lowest-energy conformation with the DOPE module. Each triazole compound was modelled using the Builder module in Pymol (http://www.py-mol.org/), based on the bound structure of colchicine in the crystal structure with pdb ID 1SA0. Each compound was modelled in a minimum of four orientations; this, followed by extensive optimization, ensured that all possible bounds states described by the configurational space around the two rotatable bonds connected to the triazole ring were explored. Subsequent optimization consistently converged to one orientation with significantly greater interaction energies with the protein than other orientations (approx. ⩾10 kcal mol^{-1}, except for the weakly binding **39–41** series). Optimization consisted of an iterative procedure. Initially, the protein conformation was constrained, and 1000 steps of steepest des-

cent (SD) energy minimization of the ligand was performed, before the constraints were released, and a further 1000 SD steps were carried out. Subsequently, ten rounds of 1000-step adopted basis Newton-Raphson (ABNR) minimization were performed, and the overall system potential energy and protein-ligand interaction energies were followed to ensure convergence. Finally, a further 1000-step SD minimization was performed, and the protein-ligand interaction energy and its component contributions were recorded. Each protein-ligand complex was optimized in the CHARMM program, using the CHARMM27/CMAP protein parameters, and the CHARMM CGenFF general force field for the triazole compounds, with non-bonded exclusions for 1–2, 1–3, and 1–4 bonded atoms. Non-bonded interactions were treated with an atom-based cutoff of 1.4 nm. Electrostatics used a distance-dependent dielectric, with a shifted potential going to zero beyond 1.2 nm. Van der Waal's forces were switched from 1.0 nm to 1.2 nm. Visual analysis was performed using VMD (http://www.ks.uiuc.edu/Research/vmd/), and data was analyzed with Grace (http://plasma-gate.weizmann.ac.il/Grace/).

Acknowledgments

Supplementary data

Supplementary data associated with this article can be found, in the online version, at doi:10.1016/j.bmc.2012.01.010.

References and notes

1. Siemann, D. W. *Cancer Treat. Rev.* **2011**, *37*, 63.
2. (a) Dumontet, C.; Jordan, M. A. *Nat. Rev. Drug Discov.* **2010**, *9*, 790; (b) Heath, V. L.; Bicknell, R. *Nat. Rev. Clin. Oncol.* **2009**, *6*, 395; (c) Remick, S. C.; Nagaiah, G. *Future Oncol.* **2010**, *6*, 1219.
3. (a) Pettit, G. R.; Singh, S. B.; Hamel, E.; Lin, C. M.; Alberts, D. S.; Garcia-Kendall, D. *Experientia* **1989**, *45*, 209; (b) Pettit, G. R.; Singh, S. B.; Niven, M. L.; Hamel, E.; Schmidt, J. M. *J. Nat. Prod.* **1987**, *50*, 119; (c) Cirla, A.; Mann, J. *Nat. Prod. Rep.* **2003**, *20*, 558.
4. (a) Busk, M.; Bohn, A. B.; Skals, M.; Wang, T.; Horsman, M. R. *Vascul. Pharmacol.* **2011**, *54*, 13; (b) van Heeckeren, W. J.; Bhakta, S.; Ortiz, J.; Duerk, J.; Cooney, M. M.; Dowlati, A.; McCrae, K.; Remick, S. C. *J. Clin. Oncol.* **2006**, *24*, 1485.
5. Hasani, A.; Leighl, N. *Clin. Lung Cancer* **2011**, *12*, 18.
6. Kumaran, G. C.; Jayson, G. C.; Clamp, A. R. *Br. J. Cancer* **2009**, *100*, 1.
7. (a) Shan, Y.; Zhang, J.; Liu, Z.; Wang, M.; Dong, Y. *Curr. Med. Chem.* **2011**, *18*, 523; (b) Singh, S. R.; Kaur, H. *Synthesis* **2009**, 2471; (c) Bhattacharyya, B.; Panda, D.; Gupta, S.; Banerjee, M. *Med. Res. Rev.* **2008**, *28*, 155; (d) Tron, G. C.; Pirali, T.; Sorba, G.; Pagliai, F.; Busacca, S.; Genazzani, A. A. *J. Med. Chem.* **2006**, *49*, 3033. and references cited therein.
8. (a) Ravelli, R. B. G.; Gigant, B.; Curmi, P. A.; Jourdain, I.; Lachkar, S.; Sobel, A.; Knossow, M. *Nature* **2004**, *428*, 198; (b) Lin, C. M.; Ho, H. H.; Pettit, G. R.; Hamel, E. *Biochemistry* **1989**, *28*, 6984.
9. Beale, T. M.; Myers, R. M.; Shearman, J. W.; Charnock-Jones, D. S.; Brenton, J. D.; Gergely, F. V.; Ley, S. V. *Med. Chem. Commun.* **2010**, *1*, 202.
10. Brown, T.; Holt, H., Jr.; Lee, M. *Top. Heterocycl. Chem.* **2006**, *2*, 1.
11. For the purpose of the following discussion, 1,5-geometry of triazoles refers to compounds in which the two aromatic components are vicinal, which neglects IUPAC nomenclature for some compounds. 1,4-geometry refers to triazoles in which the aromatic groups are not on adjacent atoms.
12. Odlo, K.; Hentzen, J.; Dit Chabert, J. F.; Ducki, S.; Gani, O. A.; Sylte, I.; Skrede, M.; Flørenes, V. A.; Hansen, T. V. *Bioorg. Med. Chem.* **2008**, *16*, 4829.
13. Cafici, L.; Pirali, T.; Condorelli, F.; Del Grosso, E.; Massarotti, A.; Sorba, G.; Canonico, P. L.; Tron, G. C.; Genazzani, A. A. *J. Comb. Chem.* **2008**, *10*, 732.
14. Odlo, K.; Hentzen, J.; Dit Chabert, J. F.; Ducki, S.; Gani, O. A.; Sylte, I.; Hansen, T. V. *Bioorg. Med. Chem.* **2010**, *18*, 6874.
15. Pati, H. N.; Wicks, M.; Holt, H. L., Jr.; LeBlanc, R.; Weisbruch, P.; Forrest, L.; Lee, M. *Heterocycl. Commun.* **2005**, *11*, 117.
16. Zhang, Q.; Peng, Y.; Wang, X. I.; Keenan, S. M.; Arora, S.; Welsh, W. J. *J. Med. Chem.* **2007**, *50*, 749.
17. Romagnoli, R.; Baraldi, P. G.; Cruz-Lopez, O.; Cara, C. L.; Carrion, M. D.; Brancale, A.; Hamel, E.; Chen, L.; Bortolozzi, R.; Basso, G.; Viola, G. *J. Med. Chem.* **2010**, *53*, 4248.
18. Semenov, V. V.; Kiselyov, A. S.; Titov, I. Y.; Sagamanova, I. K.; Ikizalp, N. N.; Chernysheva, N. B.; Tsyganov, D. V.; Konyushkin, L. D.; Firgang, S. I.; Semenov, R. V.; Karmanova, I. B.; Raihstat, M. M.; Semenova, M. N. *J. Nat. Prod.* **2010**, *73*, 1796.
19. Akselsen, Ø. W.; Odlo, K.; Cheng, J.-J.; Maccari, G.; Botta, M.; Hansen, T. V. *Bioorg. Med. Chem.* **2011**. doi:10.1016/j.bmc.2011.11.010.
20. (a) Shearman, J. W.; Myers, R. M.; Beale, T. M.; Brenton, J. D.; Ley, S. V. *Tetrahedron Lett.* **2010**, *51*, 4812; (b) Shearman, J. W.; Myers, R. M.; Brenton, J. D.; Ley, S. V. *Org. Biomol. Chem.* **2011**, *9*, 62; (c) Manzo, E.; van Soest, R.; Matainaho, L.; Roberge, M.; Andersen, R. J. *Org. Lett.* **2003**, *5*, 4591.
21. Schobert, R.; Biersack, B.; Dietrich, A.; Effenberger, K.; Knauer, S.; Mueller, T. *J. Med. Chem.* **2010**, *53*, 6595.
22. Wang, L.; Woods, K. W.; Li, Q.; Barr, K. J.; McCroskey, R. W.; Hannick, S. M.; Gherke, L.; Bruce Credo, R.; Hui, Y.-H.; Marsh, K.; Warner, R.; Lee, J. Y.; Zielinski-Mozng, N.; Frost, D.; Rosenberg, S. H.; Sham, H. L. *J. Med. Chem.* **2002**, *45*, 1697.
23. Biersack, B.; Muthukumar, Y.; Schobert, R.; Sasse, F. *Bioorg. Med. Chem. Lett.* **2011**, *21*, 6270.
24. Pagliai, F.; Pirali, T.; Del Grosso, E.; Di Brisco, R.; Tron, G. C.; Sorba, G.; Genazzani, A. A. *J. Med. Chem.* **2006**, *49*, 467.
25. Lista, L.; Pezzella, A.; Napolitano, A.; d'Ischia, M. *Tetrahedron* **2008**, *64*, 234.
26. Colvin, E. W.; Hamill, B. J. *J. Chem. Soc. Perkin Trans.* **1977**, *1*, 869.
27. Kaisalo, L.; Latvala, A.; Hase, T. *Synth. Commun.* **1986**, *16*, 645.
28. Boren, B. C.; Narayan, S.; Rasmussen, L. K.; Zhang, L.; Zhao, H.; Lin, Z.; Jia, G.; Fokin, V. V. *J. Am. Chem. Soc.* **2008**, *130*, 8923.
29. (a) Pettit, G. R.; Thornhill, A.; Melody, N.; Knight, J. C. *J. Nat. Prod.* **2009**, *72*, 380; (b) Pettit, G. R.; Lippert, J. W., III; Herald, D. L.; Hamel, E.; Pettit, R. K. *J. Nat. Prod.* **2000**, *63*, 969.
30. CA–1 (3) was synthesised according to literature procedure **3b** and assayed immediately after characterisation.
31. Pettit, G. R.; Thornhill, A. J.; Moser, B. R.; Hogan, F. *J. Nat. Prod.* **2008**, *71*, 1561.
32. Compounds stable in DMSO solution for up to 18 months, shown by LC-MS analysis.
33. Eswar, N.; Marti-Renom, M. A.; Webb, B.; Madhusudhan, M. S.; Eramian, D.; Shen, M.; Pieper, U.; Sali, A. Current Protocols in Bioinformatics, John Wiley & Sons Inc., Supplement 15 2006, 5.6.1–5.6.30.
34. Brooks, B. R.; Brooks, C. L., III; Mackerell, A. D.; Nilsson, L.; Petrella, R. J.; Roux, B.; Won, Y.; Archontis, G.; Bartels, C.; Boresch, S.; Caflisch, A.; Caves, L.; Cui, Q.; Dinner, A. R.; Feig, M.; Fischer, S.; Gao, J.; Hodoscek, M.; Im, W.; Kuczera, K.; Lazaridis, T.; Ma, J.; Ovchinnikov, V.; Paci, E.; Pastor, R. W.; Post, C. B.; Pu, J. Z.; Schaefer, M.; Tidor, B.; Venable, R. M.; Woodcock, H. L.; Wu, X.; Yang, W.; York, D. M.; Karplus, M. *J. Comp. Chem.* **2009**, *30*, 1545.
35. Mackerell, A. D.; Bashford, D.; Bellott, M.; Dunbrack, R. L.; Evanseck, J. D.; Field, M. J.; Fisher, S.; Gao, J.; Guo, H.; Ha, S.; Joseph-McCarthy, D.; Kuchnir, L.; Kuczera, K.; Lau, F. T. K.; Mattos, C.; Michnick, S.; Ngo, T.; Nguyen, D. T.; Prodhom, B.; Reiher, W. E., III; Roux, B.; Schlenkrich, M.; Smith, J. C.; Stote, R.; Straub, J.; Watanabe, M.; Wiorkiwicz-Kuczera, J.; Yin, D.; Karplus, M. *J. Phys. Chem. B* **1998**, *102*, 3586.
36. Vabommeslaeghe, K.; Hatcher, E.; Acharya, C.; Kundu, S.; Zhong, S.; Shim, J.; Darian, E.; Guvench, O.; Lopes, P.; Vorobyov, I.; Mackerell, A. D. *J. Comput. Chem.* **2010**, *31*, 671.
37. Kita, Y.; Tohma, H.; Hatanaka, K.; Takada, T.; Fujita, S.; Mitoh, S.; Sakurai, H.; Oka, S. *J. Am. Chem. Soc.* **1994**, *116*, 3684.
38. Pettit, G. R.; Singh, S. B.; Cragg, G. M. *J. Org. Chem.* **1985**, *50*, 3404.
39. Mattson, A. E.; Scheidt, K. A. *J. Am. Chem. Soc.* **2007**, *129*, 4508.
40. Ritz, C.; Streibig, J. C. *J. Statist. Software* **2005**, *12*.
41. R Development Core Team. **2010**, http://www.R-project.org/.